Hindawi
Shock and Vibration
Volume 2021, Article ID 5533086, 12 pages
https://doi.org/10.1155/2021/5533086

Research Article

Rheological Properties of Argillaceous Intercalation under the Combination of Static and Intermittent Dynamic Shear Loads

Xin Zhang,[1] **Qian Dong**,[2,3] **Xiangping Zhang**,[1] **Ming Lang**,[1] **Suzhi Zhao**,[1] **Zhuoang Chen**,[2,3] **and Jinshan Sun**[2,3]

[1]*China Railway 18 Bureau Group Co.,Ltd, Tianjin 300222, China*
[2]*Hubei Key Laboratory of Blasting Engineering, Jianghan University, Wuhan, Hubei 430056, China*
[3]*Hubei (Wuhan) Institute of Explosion Science and Blasting Technology, Jianghan University, Wuhan, Hubei 430056, China*

Correspondence should be addressed to Jinshan Sun; sunjinshan@cug.edu.cn

Received 21 January 2021; Accepted 28 July 2021; Published 9 August 2021

Academic Editor: Francesco Bucchi

The construction and long-term operation stage of the rock slope with argillaceous interlayer will be subjected to intermittent dynamic loads, such as blasting and earthquake. For the argillaceous interlayer in the rock slope, its rheological properties are not only related to the initial stress state caused by the gravity of the overlying rock mass but also affected by intermittent dynamic loads. In order to investigate the rheological properties of argillaceous intercalation under the combination of static and intermittent dynamic shear loads, the rheological tests of argillic intercalated soil samples under static shear, static and cyclic dynamic shear, and static and intermittent dynamic shear were carried out, and the rheological deformation characteristics of soil samples under different shear conditions were analyzed. The results show that when the soil specimens in the static shear rheological process are disturbed by intermittent dynamic shearing load, the intermittent dynamic disturbances might have no remarkable influence on the rheological deformation of the specimens if the initial static shearing stress and intermittent dynamic shearing stress were comparatively low. However, low-intensity intermittent dynamic disturbances might accelerate the rheological deformation process of the specimens remarkably if the initial static shearing stress state was close to their shearing strength. There was a stress threshold when the soil specimens failed under the static and cycling dynamic shear and static and intermittent dynamic shear, which is determined by the sum of static shear stress and dynamic shear stress peak. For rock slopes controlled by rheological weak structural planes and influenced by long-term blasting vibrations, the transient and long-term dynamic stability should be comprehensively analyzed.

1. Introduction

There are inevitably a certain number of weak structural planes in natural rock slope, which control their mechanical response and stability [1–5]. Under the natural actions, such as self-weight, rainfall, and earthquake, rock slopes often slide along these weak structural planes and induce landslide disaster. Usually, these weak structural planes have obvious rheological properties, and their mechanical parameters will deteriorate under dynamic loads such as earthquake and blasting excavation, which lead to rheological deformation and progressive instability of rock slope [6, 7]. Therefore, it is of great theoretical and practical significance to study the rheological properties of weak structural planes under dynamic loads for improving the long-term stability of rock slope and avoiding landslide failure.

It is well known that the vibration induced by blasting excavation has adverse effects on the surrounding buildings and equipment [8, 9]. At the same time, the dynamic loads of rock slope, such as earthquake or blasting excavation, are mostly long-term or periodic [10, 11]. In sum, the effects of intermittent dynamic loads on weak interlayer are mainly the accumulation of instantaneous damage and the change of long-term deformation characteristics.

Intensive research had been carried out on the cumulative damage of rock or structural planes caused by

intermittent or multiple dynamic loads [12–16]. For example, Li et al. [17] adopted the restart function of the finite element software ANSYS/LS-DYNA to explore the evolution mechanism and distribution law of rock cumulative damage under cyclic blasting. Liu et al. [18] studied the cumulative damage and failure mode of horizontal layered rock slope subjected to seismic loads. Cao et al. [19] built on the HJC constitutive model to study the effects of cyclic blast loading on shared rock in a neighborhood tunnel. Chai et al. [20] conducted a dynamic impact test to study on dynamic compression characteristics of rock with filled joints after cumulative damage. Song et al. [21] utilized the ground penetrating radar to detect the surrounding rock cumulative damage during tunnel blasting excavation.

On the other hand, because the rheology of weak discontinuities has a great influence on the long-term stability of geotechnical engineering, some scholars had systematically studied the rheological characteristics of weak discontinuities under static loads [22–24], but there are few studies on its rheology under dynamic disturbance. For example, Šancer et al. [25] presented some results of the laboratory tests on the time-dependent behavior of three types of sandstone and focused on the rheological rock properties during vibration (cyclic) loading. Hu et al. [26, 27] studied the dynamic rheological parameters of sludge soft soil through dynamic shear tests, and the rheological mechanism characteristics and rheological parameters of sludge soft soil under dynamic loading were deduced.

To sum up, the rock slopes formed by the open-pit mine, water conservancy and hydropower engineering, large-scale building foundation pit, and so on are often disturbed by blasting seismic effect for a long time. However, there are few studies on the influence of dynamic disturbances on the rheological process of weak structural planes of slope, so that the static evaluation methods are still mainly used to evaluate the long-term stability of rock slope, and only the transient stability analysis method is used to evaluate the dynamic stability of slope. For this reason, this paper has carried out preliminary laboratory test research on the rock slope controlled by the weak structural planes under the long-term disturbances of blasting excavation, and the shear rheological characteristics of the weak mud interlayer under the intermittent cyclic dynamic load were analyzed.

2. Influence Mechanism Analysis

The weak structural planes generally refer to the geological structural planes with weak shear strength, such as fault fracture zones and weak interlayers. There are many types of soft structural planes, and their properties are complex. Among them, the filling weak structures planes have wide distribution, low strength, and significant rheological properties and are sensitive to blasting vibration.

Therefore, the representative thin-layered muddy interlayers were selected in this paper. In the rock slope, the soft structural planes are always subjected to the gravity of the overlying strata, which can lead to normal stress and tangential stress on the structural planes. When the production blasting excavation was carried out in a rock slope as shown in Figure 1(a), the incidental blasting seismic waves will cause the overlying rock mass on the structural surface to bear two horizontal and one vertical seismic inertial forces. If the intensity of blasting excavation is high, or under the action of long-term cyclic blasting loads, the strength of muddy interlayers will be decreased, which will eventually lead to landslide hazard on the slope, as shown in Figure 1(b). After the seismic inertial forces are applied to the soft structural plane, additional dynamic stresses in the normal and tangential directions can be formed as shown in Figure 2, where σ_s, σ_d, τ_s and τ_d denote initial normal stress, additional dynamic normal stress, initial shear stress, and additional dynamic shear stress of the argillized interlayer.

The seismic inertial forces and additional dynamic stresses are mainly affected by the velocity and acceleration of rock mass vibration caused by blasting. At present, according to the Blasting Safety Regulation (GB6722-2014) in China, the safe allowable particle vibration velocity of permanent rock slope is 5~15 cm/s (vibration frequency 10~100 Hz). According to the theoretical conversion, the relation between vibration velocity v and acceleration a is as follows:

$$a = 2\pi f v, \tag{1}$$

where π and f are the circumference ratio and the frequency of particle vibration velocity. The corresponding safety allowable rock mass particle acceleration value should be approximately 3~15 m/s^2. Generally, in order to ensure the stability of the rock slope, after the blasting charge is controlled, the measured particle acceleration on the surface of slope is generally about 0~3 m/s^2 (area far away from the explosion source). That is, the additional seismic inertial forces are about 0~0.3 times the weight of the overlying rock mass, so the peak value of the additional dynamic stresses in the normal and tangential directions is also about 0~0.3 times the static normal and tangential stresses.

3. Experimental Methods

In order to study the influence of blasting vibration on the soft argillaceous intercalations, argillic intercalated circular cake saturated soil samples were made, and rheological tests under static shear, static and cyclic dynamic shear, and static and intermittent dynamic shear were carried out on those samples with a direct-shear rheometer attached with dynamic loads.

3.1. Test Instrument. The ZLB-1 triple rheological direct shear tester (Figure 3) produced by Nanjing Soil Instrument Factory was used in the test. The instrument applies certain normal pressures on the soil samples and a shear force on the shear surface to test the shear deformation of the samples. The diameter and height of the specimen corresponding to the equipment are 61.8 mm and 20 mm, respectively, and the maximum shear and normal force provided by the instrument are both 1.8 kN. An electromagnet controlled by a signal generator was installed at the bottom of the instrument weight to apply a simple harmonic vibration load, and an additional dynamic shear stress can be applied to the samples.

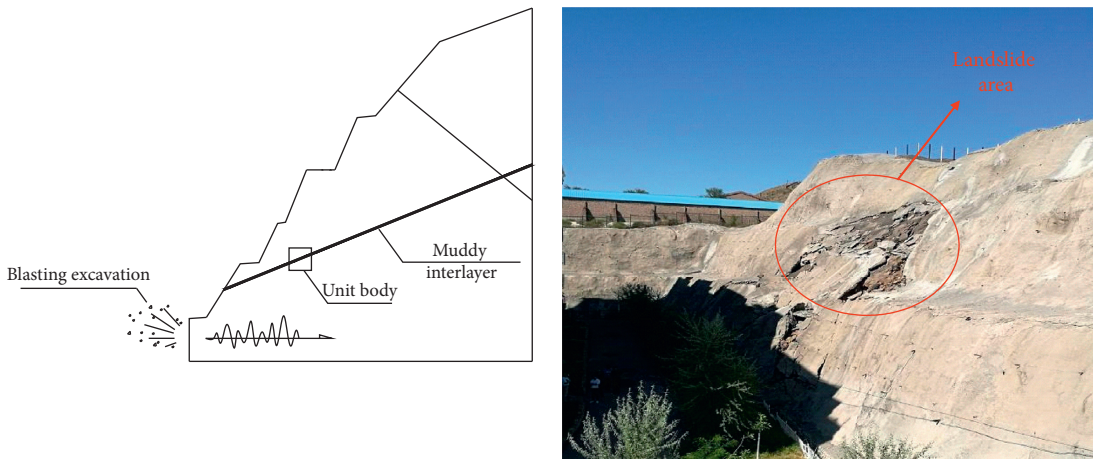

Figure 1: Rock slope with an argillaceous intercalation under blasting influence. (a) Force analysis of slope. (b) Landslide hazard.

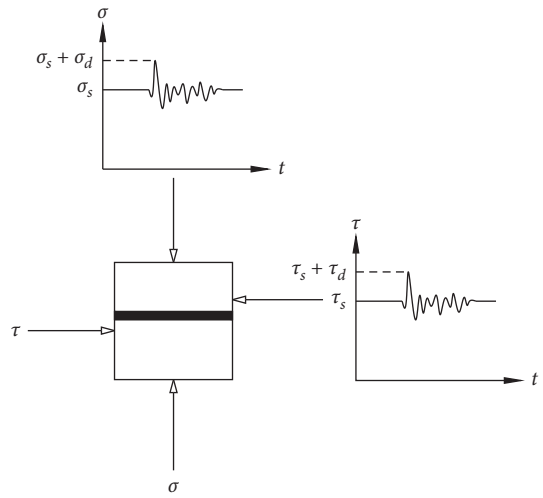

Figure 2: Stress diagram of the argillized interlayer element under blasting loads.

3.2. Soil Samples' Preparation. The soil samples were taken from a clay-like argillaceous interlayer with a thickness of 5 cm~20 cm in a quartz sandstone formation in Wuhan, a piece of it shown in Figure 4(a), and the standard shear test specimens with the diameter $D = 61.8$ mm and the thickness $H = 20$ mm were made matching with test equipment as shown in Figure 4(b). The physical and mechanical parameters of the soil samples are shown in Table 1.

3.3. Experimental Procedure. Shear rheological tests under static shear, static and cyclic dynamic shear, and static and intermittent dynamic shear were conducted for the prepared soil specimens. Before the test, apply pressure to the specimens in the shear box of the rheological direct shear apparatus for consolidation, and it lasts for 24 h. The detailed procedure of the three experiments conducted is shown below.

(1) Static shear rheological test: three soil samples were made, and the permeable rocks were immersed in water. Rubber film was sandwiched between the permeable rocks and the samples. After the samples were consolidated for 24 hours under a shear stress of 22.5 kPa and a normal pressure of 150 kPa, the shear stress increased to 25 kPa, 32 kPa, and 38 kPa, which are 60%, 75%, and 90% of its ultimate shear stress, respectively. The rheological deformation characteristics of the samples were observed after the static loads were applied and remained unchanged.

(2) Static and cyclic dynamic shear rheological test: three sets of three soil samples were made, a total of nine specimens. After consolidation for 24 hours under the stress state of 150 kPa normal pressure and 22.5 kPa shear stress, the shear stress of three groups of samples is loaded to its ultimate shear stress at 60%, 75%, and 90%, respectively, and then each

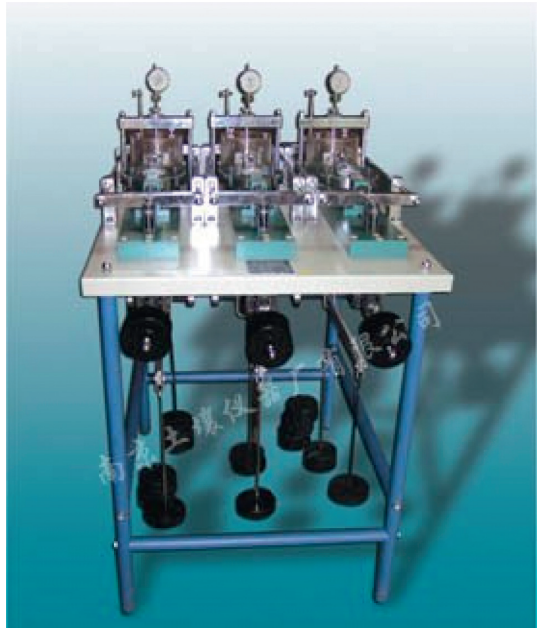

Figure 3: The ZLB-1 creep shear apparatus.

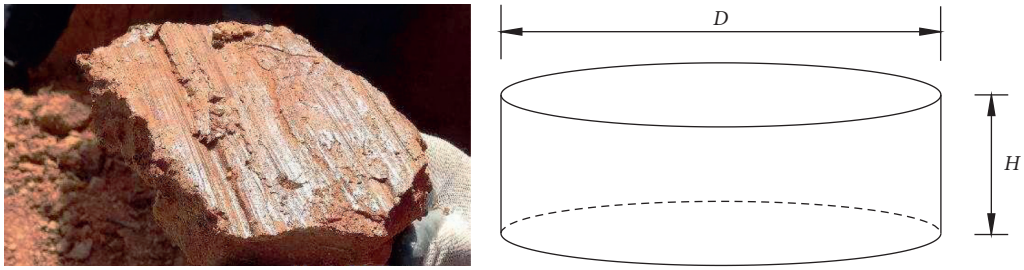

(a) (b)

Figure 4: Preparation of soil samples. (a) A piece of the argillaceous interlayer. (b) Soil sample size illustration.

Table 1: Parameters of the soil specimens.

Parameters	Values
Density	1.85 g/cm^3
Void ratio	0.82
Moisture content	24.8%
Saturation	81.9%
Cohesive force	5.0 kPa
Friction angle	14°

group of samples exerted the dynamic shear loads of 30 Hz frequency, and the corresponding peak values were 2.1 kPa, 4.2 kPa, and 8.5 kPa in the form of a sine wave, so the peak shear stresses caused by the dynamic loads were approximately 5%, 10%, and 20% of the ultimate shear stress, respectively. The maximum deformation was measured after applying the dynamic loads for 30 s and suspended for another 30 s.

(3) Static and intermittent dynamic shear rheological stress: the preparation and consolidation process of the soil samples and the initial static shear state were the same as the static and cyclic dynamic shear rheological test. Then, the 30 Hz frequency dynamic shear loads of the peak values were 2.1 kPa, 4.2 kPa, and 8.5 kPa, and in the form of a sine wave, they were applied. In the practical engineering, the dynamic disturbance of blasting was generally once a day. In order to shorten the test time, the dynamic disturbances were five times a day at 9:00, 12:00, 15:00, 18:00, and 21:00, respectively, and the duration time of each disturbance was 1 s.

4. Results and Analysis

4.1. Static Shear Rheological Characteristics of Argillaceous Intercalation. According to the test scheme, after the soil specimens were consolidated for 24 hours under the action of normal pressure and shear stress, the deformation was measured after the shear stress increased, and then the value of strain is 0. Therefore, the shear deformation curves (Figure 5) contain the elastic deformation increment of

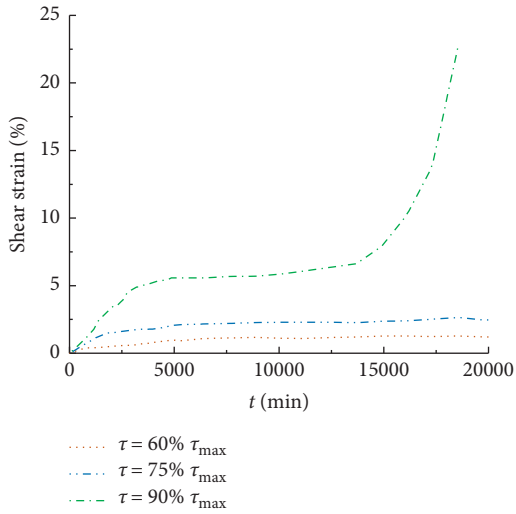

Figure 5: Strain of specimens under static shear load.

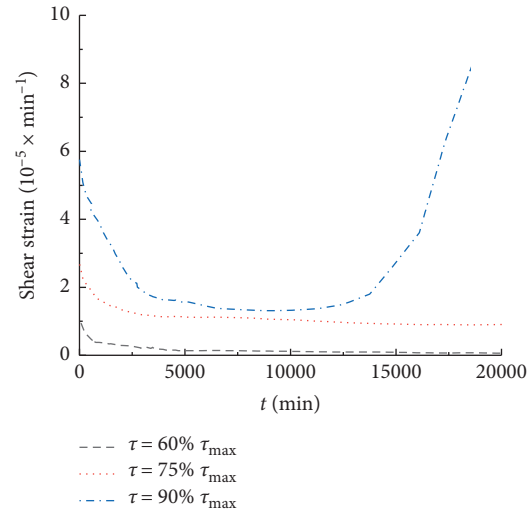

Figure 6: Rheological strain rate curves of specimens under static shear stress.

samples. However, in the test process, the shear strain of the three samples also increased rapidly after the sudden increase of shear stress. Because the shear stress increment was relatively small, the sudden increase of deformation increment was within 0.03 mm, and the shear strain was within 0.5%, so the elastic deformation increment was small, which was not significant. Therefore, the rheological deformation of the samples can be shown in Figure 5.

After the elastic deformation stage, two specimens with shear stress τ of 60% τ_{max} (ultimate shear stress) and 75% τ_{max}, the deformation gradually increased with the time passing within the first 5000 mins, and the shear strain was less than 2%. After 5000 mins, the increase of deformation is not significant, and the specimens did not break during the test, so their deformation may be mainly viscoelastic deformation.

When the specimen shear stress τ is 90% τ_{max}, the shear strain of the specimen in the first 5000 mins continues to increase, dominated by the viscoelastic deformation. The increase in strain is lower during 5000 mins~15000 mins, but the strain increases rapidly after 15000 mins until the specimen was broken, and the deformation at this stage is mainly plastic deformation.

According to the shear rheological curves, the deformation increments of the samples were counted every 10 mins to obtain the rheological rate curves of the samples (Figure 6). Since the elastic deformation is small, it is included in the deformation increment of the first 10 mins and counted together. The statistical results show that the deformation rate of the three samples within the first 1000 mins is relatively fast, and the deformation rate of the sample with τ of 90% τ_{max} is the fastest, and the sample with τ of 60% τ_{max} is the slowest.

Subsequently, the rheological rate of the samples decreased rapidly. After 10,000 mins, the rheological rate of the sample with $\tau = 60\%\ \tau_{max}$ was close to 0, while the rheological rates of the samples with $\tau = 75\%\ \tau_{max}$ and $\tau = 90\%\ \tau_{max}$ were still higher and become closer. The strain rate of the specimen with shear stress $\tau = 90\%\ \tau_{max}$ increased rapidly after 15,000 mins and had been in an accelerated deformation state before failure, while the strain rate of specimen with $\tau = 75\%\ \tau_{max}$ continued to decrease.

It can be preliminarily inferred from the test results that when the normal stress is 150 kPa, the long-term shear strength τ_{cr} of the soil samples may be a value between 75% τ_{max} and 90% τ_{max}, namely,

$$75\%\ \tau_{max} < \tau_{cr} < 90\%\ \tau_{max}. \quad (2)$$

However, due to the limitations of the quantity of test samples and the static loading capacity of the instrument, this value cannot be further determined accurately. When the shear stress is less than the critical value, the attenuative creep will occur, and only when the static load is greater than the critical value, it will lead to the final failure.

4.2. Static and Cyclic Dynamic Shear Rheological Characteristics of Argillaceous Intercalation. In the static and cyclic dynamic shear test, additional dynamic shear stresses of different strength were applied to the samples in different static shear stress states, and the strain of soil samples varied with the increase of cyclic times. The shear strain of soil samples is closely related to the cyclic dynamic shear stress and their initial static shear stress state.

When the initial shear stress of the specimens is low, such that its initial shear stress is 60% of the ultimate strength, namely, the $\tau = 60\%\ \tau_{max}$ (shown in Figure 7(a)), and the cyclic dynamic shear stress for the ultimate shear strength of 5% and 10%, namely, $\Delta\tau_p = 5\%\ \tau_{max}$ and $\Delta\tau_p = 10\%\ \tau_{max}$, the shear strain of the soil samples increased rapidly after the first few cycles of loading and then remained stable. When $\Delta\tau_p = 20\%\ \tau_{max}$, the increment of strain firstly increased rapidly and then slowed down. After 120,000 disturbances were applied, no damage occurred, and the total strain was less than 1%.

When the initial shear stress of the specimens is high, such as 90% of the ultimate strength, namely, $\tau = 90\%\ \tau_{max}$, even if the cyclic shear stress peak value $\Delta\tau_p$ is small, such as

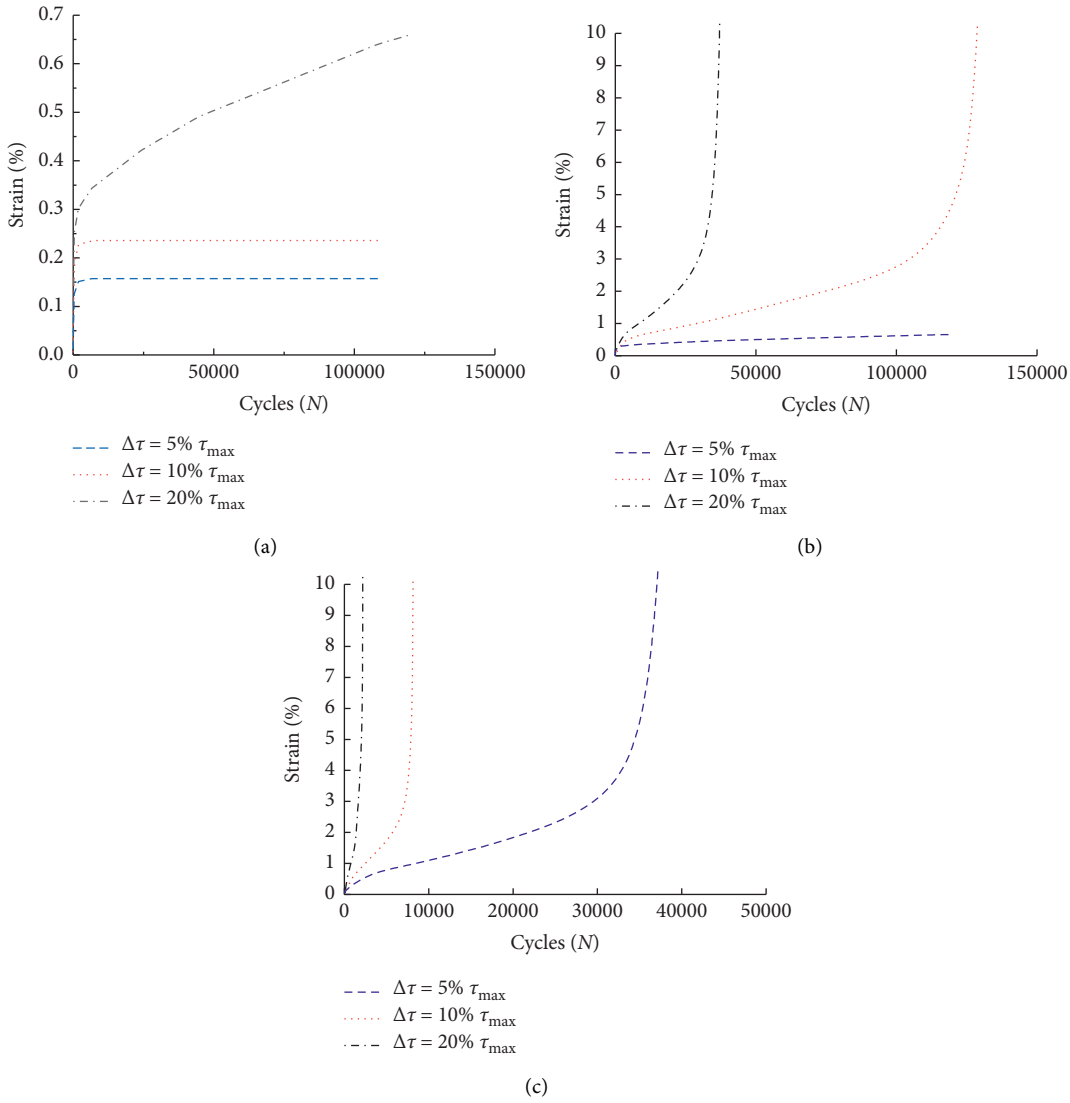

FIGURE 7: Rheological shearing strain curves under static and cyclic dynamic shear loads. (a) Specimen of $\tau = 60\%\ \tau_{max}$. (b) Specimen of $\tau = 75\%\ \tau_{max}$. (c) Specimen of $\tau = 90\%\ \tau_{max}$.

5% of its ultimate shear strength ($\Delta\tau_p = 5\%\ \tau_{max}$) (shown in Figure 7(c)), the soil samples will also be damaged after enough cyclic times, and their strain increased slowly first and then rapidly. When the dynamic stress is relatively high, such as $\Delta\tau_p = 20\%\ \tau_{max}$ (as shown in Figure 7(c)), the strain basically maintained a trend of continuous acceleration.

When the initial shear stress of the samples is at a medium level, for example, 75% of the ultimate strength (Figure 7(b)), that is, $\tau = 75\%\ \tau_{max}$, the strain variation of soil samples was more sensitive to the change of cyclic dynamic shear stress. When the dynamic shear stress is small (such as $\Delta\tau_p = 5\%\ \tau_{max}$), the strain of the soil samples increased slowly, and the final strain rate decreased to 0. When the dynamic shear stress is high (such as $\Delta\tau_p = 20\%\ \tau_{max}$), the soil samples may undergo shear failure quickly.

The test results showed that when the frequency of the dynamic shear stress is the same, and the sum of the initial static stress and the peak dynamic stress of the samples is close, the deformation characteristics of the samples were also similar. For example, the specimens with $\tau = 60\%\ \tau_{max}$, $\Delta\tau_p = 20\%\ \tau_{max}$ and $\tau = 75\%\ \tau_{max}$, $\Delta\tau_p = 5\%\ \tau_{max}$, after 120,000 times cyclic shear dynamic loads, the strains were 0.66% and 0.82%, respectively, while the specimens with $\tau = 75\%\ \tau_{max}$, $\Delta\tau_p = 20\%\ \tau_{max}$ and $\tau = 90\%\ \tau_{max}$, $\Delta\tau_p = 5\%\ \tau_{max}$ were failed after 37,800 and 33,000 times cyclic shear dynamic loads, respectively, and the variations of specimens strain were also similar.

Secondly, the failure of the samples under cyclic dynamic shear also had a certain critical value of stress state, and the samples breakage under additional dynamic stress can only occur if the total shear stress is larger than this critical value. The stress critical value (the sum of static shear stress and dynamic shear stress peak) of the soil samples should be between 70% and 80% of the shear strength, namely,

$$70\%\ \tau_{max} < \left(\tau + \Delta\tau_p\right)cr < 80\%\ \tau_{max}. \quad (3)$$

4.3. Static and Intermittent Dynamic Shear Rheological Characteristics of Argillaceous Intercalation. Intermittent dynamic shear loads were applied 5 times a day to the soil samples under different initial static stress states, and the rheological deformation characteristics of samples were observed. Compared with static rheological process, the deformation process of the samples after intermittent dynamic shear loads changed significantly.

(1) When the initial static shear stress and the intermittent dynamic shear stress were relatively low, the rheological process of the samples is similar to the static rheological process, as shown in Figure 8(a) for the sample with $\tau = 60\%\ \tau_{max}$ and $\Delta\tau_p = 5\%\ \tau_{max}$. In this way, after the rapid increase of strain in the initial stage, with the increase of time and the times of intermittent dynamic disturbances, the shear strain of the specimens had no obvious increasing trend. When the initial static shear stress was low, but the dynamic shear stress peak was relatively high, as shown in Figure 8(a), the samples with $\tau = 60\%\ \tau_{max}$, while $\Delta\tau_p = 10\%\ \tau_{max}$ and $\Delta\tau_p = 20\%\ \tau_{max}$, with the passing of time and increase of the number of disturbances, the strain continued to increase, and eventually failure occurred, while the specimens under static and cyclic dynamic shear did not fail, indicating that the intermittent dynamic shear loads changed the overall deformation of the specimens.

(2) When the initial static shear stress is at a medium stress level, such as $\tau = 75\%\ \tau_{max}$, the rheological deformation process of specimens was more sensitive to intermittent dynamic disturbances. When the dynamic shear stress peak is low, as shown in Figure 8(b), for the sample with $\Delta\tau_p = 5\%\ \tau_{max}$, the deformation rate in the early stage increased slowly, but it increased rapidly after a long period of time. Compared with the curves of static shear test and static and cyclic dynamic shear test, it showed a typical three-stage deformation characteristic.

(3) When the initial static shear stress is close to its ultimate strength, such as $\tau = 90\%\ \tau_{max}$, the rheological deformation process of soil specimens was very sensitive to intermittent dynamic disturbances; even when the dynamic shear stress peak is low, as shown in Figure 8(c), for the sample with $\Delta\tau_p = 5\%\ \tau_{max}$, the deformation rate of the specimen continued to grow rapidly, indicating that when it is close to the limit equilibrium, even a weak intermittent dynamic load can quickly destroy its equilibrium state.

(4) By comparing the deformation curves of each sample in Figure 8, it can be found that the dynamic shear stress also changed the rheological process of the samples. The deformation curves of the samples subjected to low static shear stress and low intermittent dynamic shear stress were relatively smooth, and it is difficult to visually distinguish the moment of disturbance on the deformation curves. However, when the samples are subjected to high static shear stress or high intermittent dynamic shear stress, the deformation of the samples jumped significantly, and the deformation curves showed a more obvious step-like shape.

The average rheological rate in the process of intermittent disturbances was analyzed by statistical the strain variables before and after the disturbance and the duration of the disturbance. When the initial static shear stress or the peak value of intermittent dynamic shear stress is small (as shown in Figure 9(a)), the rheological rate of the samples was higher at the initial stage and then remains at a lower level with irregular abrupt changes at some moments and increased to a higher level near the failure stage. With the increase of the initial static shear stress or intermittent dynamic shear stress peak (as shown in Figure 9(b)), the strain rate was relatively high at the initial stage and at the time of dynamic disturbance and gradually showed a certain regularity. However, when the initial shear stress was close to the ultimate strength, or the intermittent dynamic shear stress peak is high (as shown in Figure 9(c)), the rheological rate of the sample gradually increased, and the strain rate increased sharply during the dynamic disturbance. The time and numbers of intermittent dynamic disturbances can be clearly identified from the rheological rate curve.

In addition, when the intermittent dynamic shear stress of the samples is relatively large (as shown in Figure 9(c)), the static rheological rate between two adjacent intermittent disturbances was basically unchanged at the initial stage of the disturbance rheology, showing a stable rheological state. In the later stage of the disturbance rheological process, when the deformation speed of the specimens was accelerated, the dynamic deformation rate during disturbances increased gradually, and the static rheological rate between two adjacent disturbances also increased significantly, which was different from the smaller intermittent disturbance peak (as shown in Figure 9(a)).

Calculate the strain increment at a certain moment when the specimens were about to fail. Under the same initial static stress state, the strain increment of the static and intermittent dynamic shear rheological test and the sum strain increment of the static shear rheological test and static and cyclic dynamic shear rheological test were compared. For example, the strain at 17280 min of the sample with initial static shear stress $\tau = 60\%\ \tau_{max}$ and intermittent cyclic dynamic shear stress peak $\Delta\tau_p = 5\%\ \tau_{max}$ was sorted out, and the sample deformed for a total of 12 days and withstood 1800 dynamic disturbances. At the same time, the strain of the static rheological sample at 17280 min and the cyclic dynamic shear sample after 1800 cycles under the same initial static shear stress state were correspondingly sorted out, comparing the sum of the above strain with the static and intermittent disturbance rheological strain.

The statistical results showed (as shown in Figure 10) that when the static stress state, flow time, and number of dynamic disturbances were the same, the deformation of the sample under the static and intermittent cyclic dynamic shear disturbance was greater than the sum deformation of the static shear and static and cyclic dynamic

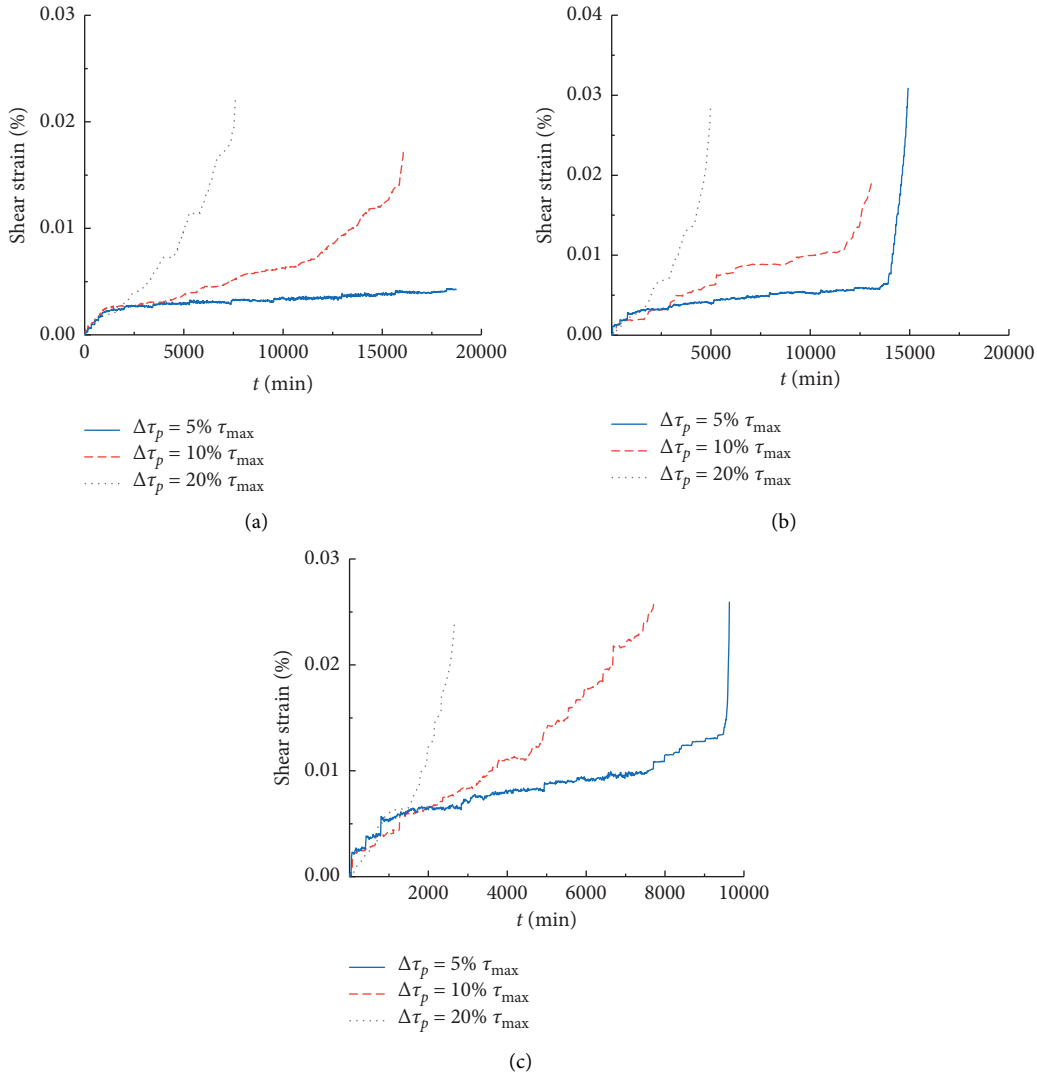

FIGURE 8: Rheological strain curves under static and intermittent dynamic shear loads. (a) Specimen of $\tau = 60\%\ \tau_{max}$. (b) Specimen of $\tau = 75\%\ \tau_{max}$. (c) Specimen of $\tau = 90\%\ \tau_{max}$.

shear. Moreover, when the samples were finally damaged, the intermittent disturbance rheological strain increment was several times that of the latter, and the closer it was to the failure moment, the more significant the difference was.

The results showed that static shear rheological deformation and intermittent cyclic dynamic shear deformation influence and promote each other. When the soil specimens approach failure, both static shear and intermittent dynamic shear promote soil damage and reduce its strength, thus making their accelerating deformation effect stronger. It can be seen that the small and transient dynamic disturbance may have a significant promoting effect on the rheological process of the argillite soft structural planes, and the greater the disturbance load is, the stronger the influence will be; meanwhile, the soil samples are more sensitive to the intermittent dynamic disturbance as it approaches the ultimate bearing state.

The duration time of the soil samples from the beginning of rheology to complete failure was defined as the rheological life time t_f. During the test, because the deformation of the samples after breakage was different, when the strain in the accelerated rheological stage reached 15%, the samples were considered to have reached their rheological life.

The relationship curves of the rheological life time t_f with the static loads and intermittent cyclic dynamic shear loads of soil samples showed that (as shown in Figure 11) the rheological life time t_f of the samples decreases with the increase of their static shear stress and intermittent dynamic shear stress, indicating that there is also a certain critical stress state that controls whether the samples can eventually be destroyed during the tests. From Figures 11 and 8(a), it can be found that when the peak value sum of static shear stress and intermittent dynamic shear stress of the soil samples is about 65% to 70% of its ultimate shear strength, the samples may eventually be damaged, namely,

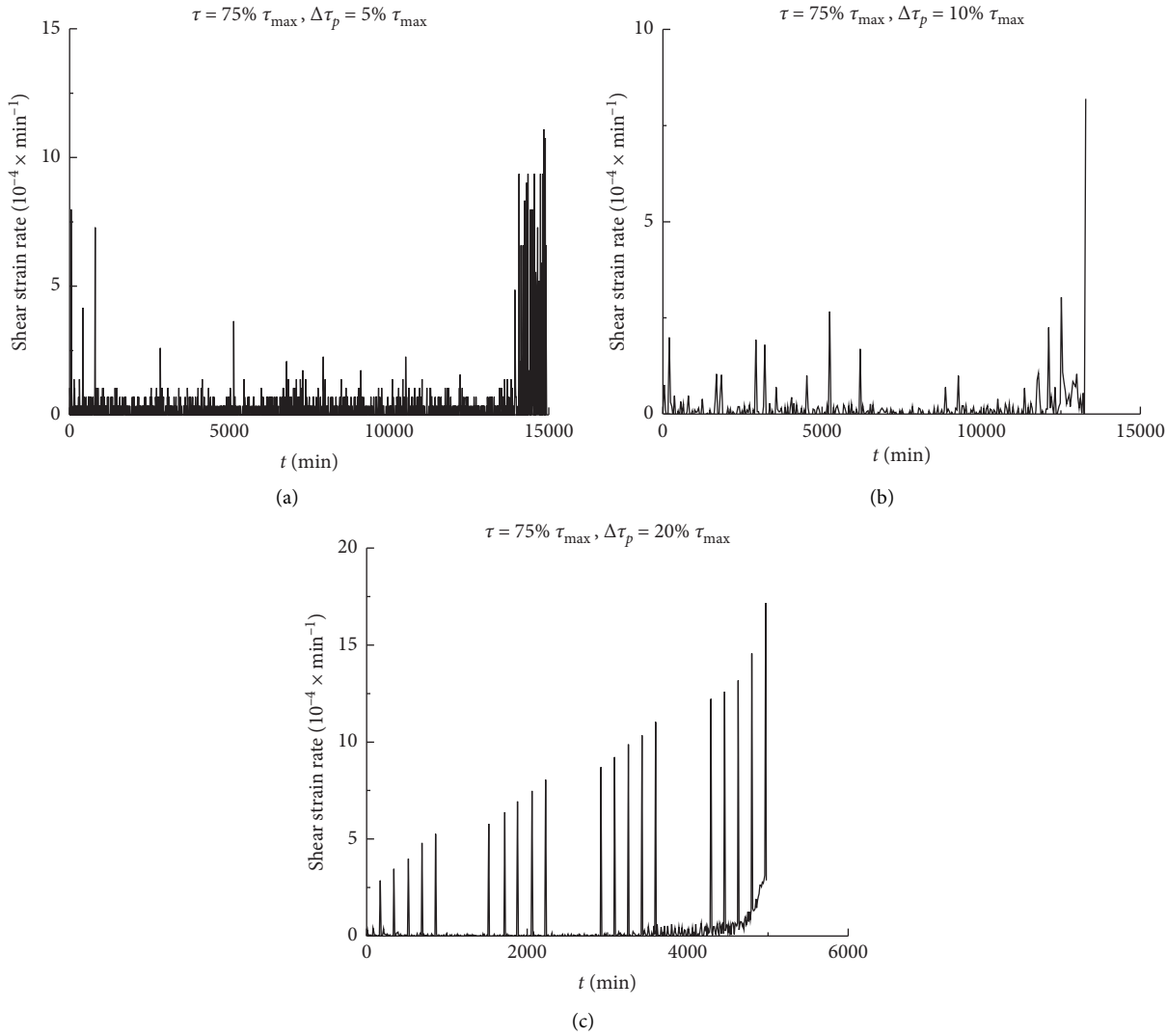

Figure 9: Rheological strain rate curves of specimens under static and intermittent dynamic shear loads ($\tau = 75\%\ \tau_{max}$). (a) $\Delta\tau_p = 5\%\ \tau_{max}$. (b) $\Delta\tau_p = 10\%\ \tau_{max}$. (c) $\Delta\tau_p = 20\%\ \tau_{max}$.

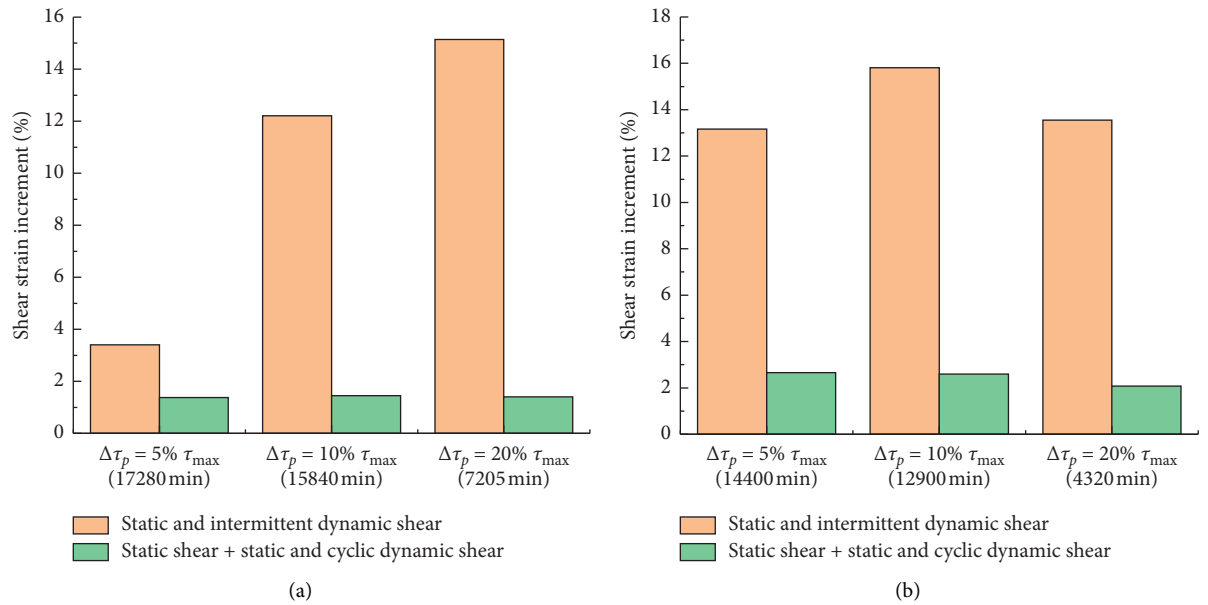

Figure 10: Continued.

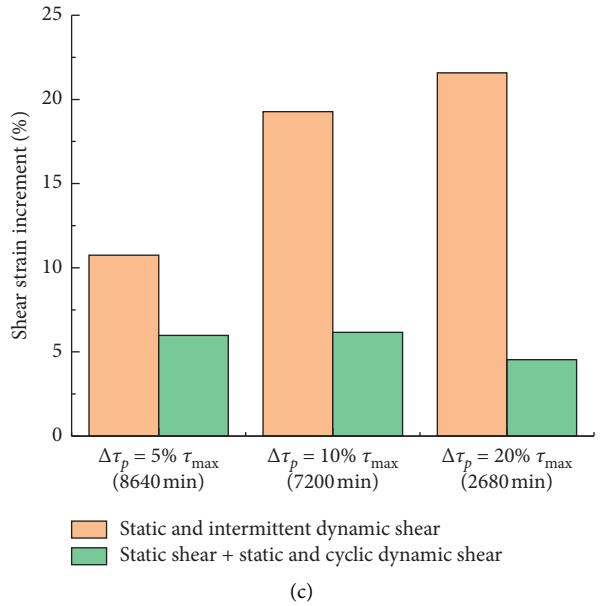

FIGURE 10: Comparison of the rheological strain increment in different shear tests. (a) Specimen of $\tau = 60\%\ \tau_{max}$. (b) Specimen of $\tau = 75\%\ \tau_{max}$. (c) Specimen of $\tau = 90\%\ \tau_{max}$.

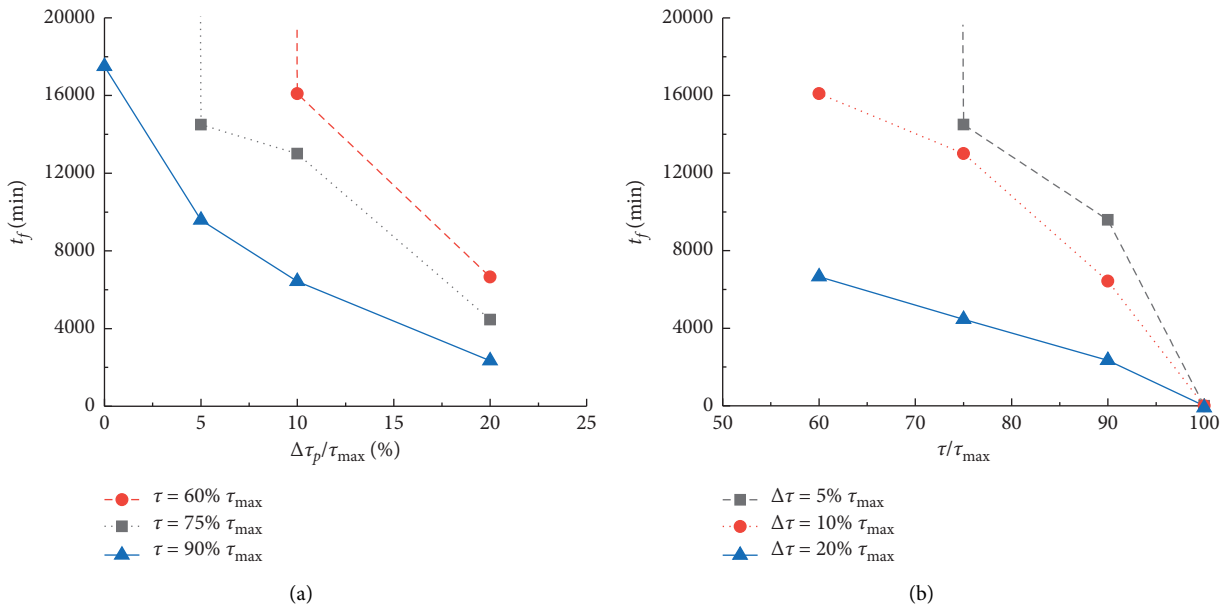

FIGURE 11: Rheological life of specimens versus static shear stress and peak value of dynamic stress. (a) Peak value of intermittent dynamic shear stress. (b) Static shear stress.

$$65\%\ \tau_{max} < \left(\tau + \Delta\tau_p\right) M_{cr} < 70\%\ \tau_{max}. \quad (4)$$

The combined stress threshold value may be slightly lower than that of the static shear test and static and cyclic dynamic shear test. The reason of this phenomenon is that, in the static and cyclic dynamic shear test, the cyclic dynamic shear loading of 30 Hz frequency was applied for 30 s and suspended for another 30 s, so 1800 cyclic dynamic shear loads can be applied per minute. Meanwhile, the test results showed that most of the soil samples had been destroyed within 150,000 cyclic dynamic shear loads, and the corresponding failure time was about 83.3 mins. However, in the static and intermittent dynamic shear test, the failure time of most soil samples was more than 5000 mins, which is about 60 times that of the static and cyclic dynamic shear test, indicating that the time of soil samples to reach failure increased obviously. In this process, static shear and intermittent dynamic shear influence and promote each other, and both induce soil damage and reduce its strength, thus making the long-term shear strength under static and

intermittent dynamic shear lower than that of static and cyclic dynamic shear. Of course, due to the discrete of the samples, the combined stress threshold value should be verified by a large number of experiments.

5. Discussion

The experimental results showed that the long-term strength and creep life of the argillaceous interlayer may be reduced under intermittent cyclic dynamic disturbances. Therefore, the dynamic disturbance caused by intermittent blasting excavation may have a significant impact on the sliding surface parameters, the overall stability, and the local stability of the rock slope controlled by the argillaceous interlayer.

However, at present, the dynamic stability analysis of large rock slopes mainly focuses on the stability at a certain moment, and this methodology is reasonable when the dynamic disturbances are weak and the static safety factor of rock slope is relatively high, but it is not suitable for the case when the rock slopes are controlled by the weak structural plane or sliding surface, and its static stability safety factor is poor. Thus, a comprehensive analysis of transient and long-term dynamic stability should be carried out for rock slopes controlled by rheological weak structural surfaces and significantly affected by blasting vibration effect.

6. Conclusion

(1) Under the static and cyclic dynamic shearing, the strain of the argillaceous interlayer samples varies with the increase of cyclic times. When the initial static shear stress and the cyclic dynamic shear stress peak are small, the influence of dynamic disturbance on their deformation is not significant. When the initial shear stresses of the samples are high, the soil strain may increase rapidly with the increase of cyclic times, even if the cyclic dynamic shear stresses are small.

(2) If the static shear stress and the peak value of the intermittent cyclic dynamic shear stress are low, the dynamic disturbance has no significant influence on the rheological deformation process of soil samples. If the initial shear stress is close to its shear strength, weak intermittent dynamic disturbance can also significantly promote the rapid growth of their rheological deformation.

(3) Under the same initial static shear stress state, the rheological deformation under the intermittent dynamic shear disturbance is greater than the sum of the static shear and static and cyclic dynamic shear, and the rheological life of the soil samples under intermittent dynamic shear disturbance may be lower than that under static shear flow.

(4) When soil samples are finally disturbed by rheological failure, there exists a stress threshold value, which is determined by the sum of static shear stress and dynamic shear stress peak values.

(5) It is suggested to totally evaluate the transient and long-term dynamic stability of rock slopes under the long-term influence of blasting excavation and controlled by rheological weak structural planes such as argillaceous interlayers.

Data Availability

The data used to support the findings of this study are available from the corresponding author upon request.

Conflicts of Interest

The authors declare that they have no conflicts of interest.

Acknowledgments

This study was supported by the Natural Science Foundation of Hubei Province, China (2020CFB428), Innovation Group Project of the Natural Science Foundation of Hubei Province, China (2020CFA043), and Key Research and Development Project of Hubei Province, China (2020BCA084).

References

[1] W. G. Pariseau, S. Puri, and S. C. Schmelter, "A new model for effects of impersistent joint sets on rock slope stability," *International Journal of Rock Mechanics and Mining Sciences*, vol. 45, no. 2, pp. 122–131, 2008.

[2] H. Wang, B. Zhang, G. Mei, and N. Xu, "A statistics-based discrete element modeling method coupled with the strength reduction method for the stability analysis of jointed rock slopes," *Engineering Geology*, vol. 264, pp. 1–14, Article ID 105247, 2020.

[3] D. Song, Z. Chen, H. Chao, Y. Ke, and W. Nie, "Numerical study on seismic response of a rock slope with discontinuities based on the time-frequency joint analysis method," *Soil Dynamics and Earthquake Engineering*, vol. 133, pp. 1–13, Article ID 106112, 2020.

[4] K. Ma, G. Liu, L. Guo, D. Zhuang, and D. S. Collins, "Deformation and stability of a discontinuity-controlled rock slope at Dagangshan hydropower station using three-dimensional discontinuous deformation analysis," *International Journal of Rock Mechanics and Mining Sciences*, vol. 130, pp. 1–19, Article ID 104313, 2020.

[5] L. Zhao, C. Yu, X. Cheng, S. Zuo, and K. Jiao, "A method for seismic stability analysis of jointed rock slopes using Barton-Bandis failure criterion," *International Journal of Rock Mechanics and Mining Sciences*, vol. 136, pp. 1–13, Article ID 104487, 2020.

[6] X. Song, J. C. Zhang, X. B. Guo et al., "Influence of blasting on the properties of weak intercalation of a layered rock slope," *International Journal of Minerals, Metallurgy and Materials*, vol. 16, no. 1, pp. 7–11, 2009.

[7] Y. Chen, J. Xu, X. Huo, and J. Wang, "Numerical simulation of dynamic damage and stability of a bedding rock slope under blasting load," *Shock and Vibration*, vol. 2019, Article ID 9616859, 13 pages, 2019.

[8] N. Jiang, B. Zhu, X. He, C. Zhou, X. Luo, and T. Wu, "Safety assessment of buried pressurized gas pipelines subject to blasting vibrations induced by metro foundation pit excavation," *Tunnelling and Underground Space Technology*, vol. 102, Article ID 103448, 2020.

[9] B. Zhu, N. Jiang, C. Zhou, X. Luo, Y. Yao, and T. Wu, "Dynamic failure behavior of buried cast iron gas pipeline with local external corrosion subjected to blasting vibration," *Journal of Natural Gas Science and Engineering*, vol. 88, Article ID 103803, 2021.

[10] T. Y. Wu, C. B. Zhou, N. Jiang et al., "Stability analysis for high-steep slope subjected to repeated blasting vibration," *Arabian Journal of Geosciences*, vol. 13, no. 828, pp. 1–12, 2020.

[11] Y.-G. Hu, M.-S. Liu, X.-X. Wu, G. Zhao, and P. Li, "Damage-vibration couple control of rock mass blasting for high rock slopes," *International Journal of Rock Mechanics and Mining Sciences*, vol. 103, pp. 137–144, 2018.

[12] M. Ramulu, A. K. Chakraborty, and T. G. Sitharam, "Damage assessment of basaltic rock mass due to repeated blasting in a railway tunnelling project - a case study," *Tunnelling and Underground Space Technology*, vol. 24, no. 2, pp. 208–221, 2009.

[13] N. Erarslan and D. J. Williams, "The damage mechanism of rock fatigue and its relationship to the fracture toughness of rocks," *International Journal of Rock Mechanics and Mining Sciences*, vol. 56, pp. 15–26, 2012.

[14] L. X. Xie, W. B. Lu, Q. B. Zhang, Q. H. Jiang, G. H. Wang, and J. Zhao, "Damage evolution mechanisms of rock in deep tunnels induced by cut blasting," *Tunnelling and Underground Space Technology*, vol. 58, pp. 257–270, 2016.

[15] L. X. Xie, Q. B. Zhang, J. C. Gu et al., "Damage evolution mechanism in production blasting excavation under different stress fields," *Simulation Modelling Practice and Theory*, vol. 97, pp. 1–14, Article ID 101969, 2019.

[16] H. Han, D. Fukuda, H. Liu et al., "FDEM simulation of rock damage evolution induced by contour blasting in the bench of tunnel at deep depth," *Tunnelling and Underground Space Technology*, vol. 103, pp. 1–16, Article ID 103495, 2020.

[17] Y. Z. Li, Z. L. Wang, Y. P. Huang et al., "Numerical study of cumulative damage effect of rock under cyclic blast loading," *Blasting*, vol. 36, no. 2, pp. 47–53, 2019.

[18] X. R. Liu, Z. Y. Deng, Y. Q. Liu et al., "Study of cumulative damage and failure mode of horizontal layered rock slope subjected to seismic loads," *Rock and Soil Mechanics*, vol. 40, no. 7, pp. 2507–2516, 2019.

[19] F. Cao, T. H. Ling, J. Li et al., "Cumulative damage feature analysis for shared rock in a neighborhood tunnel under cyclic explosion loading," *Journal of Vibration and Shock*, vol. 37, no. 23, pp. 141–148, 2018.

[20] S. B. Chai, H. Wang, Y. L. Jing et al., "Experimental study on dynamic compression characteristics of rock with filled joints after cumulative damage," *Chinese Journal of Rock Mechanics and Engineering*, vol. 39, no. 10, pp. 2025–2037, 2020.

[21] X. L. Song, W. X. Gao, J. M. Ji et al., "Influence of blasting vibration on cumulative damage of surrounding rock," *Journal of Vibration and Shock*, vol. 39, no. 24, pp. 54–62, 2020.

[22] Y. J. Cao, R. Q. Huang, H. M. Tang et al., "Experimental research on rheological characteristics of weak structural planes of high slopes in coal strata in a hydropower station," *Chinese Journal of Rock Mechanics and Engineering*, vol. 27, no. s2, pp. 3732–3739, 2008.

[23] H. J. Hou and M. R. Shen, "Rheological properties of rock mass discontinuities and trial research of its long-term strength," *Geotechnical Engineering Technique*, vol. 6, pp. 324–326, 2003.

[24] T. H. Yang, Y. Q. Rui, W. C. Zhu et al., "Rheological characteristics and long-term strength of siltized intercalation interbeded in peat mudstone," *Journal of Experimental Mechanics*, vol. 5, pp. 396–402, 2008.

[25] J. Šancer, M. Štrejbar, and A. Maleňáková, "Effects of cyclic loading on the rheological properties of sandstones," *Central European Journal of Geosciences*, vol. 3, no. 2, pp. 207–214, 2011.

[26] H. Hu, "Rheological model and rheological equation of sullage soft soil under dynamic loading," *Rock and Soil Mechanics*, vol. 28, no. 2, pp. 237–240, 2007.

[27] H. Hu, H. X. Gu, and D. R. Yu, "Research on dynamic rheological characteristics and rheologic parameters of sludge soft soil," *Rock and Soil Mechanics*, vol. 29, no. 3, pp. 696–700, 2008.